



HAL
open science

The angular pattern in the hyperfine structure of Xe I and Kr I atoms

Christophe Blondel, Cyril Drag

► **To cite this version:**

Christophe Blondel, Cyril Drag. The angular pattern in the hyperfine structure of Xe I and Kr I atoms. *Journal of Physics B: Atomic, Molecular and Optical Physics*, 2022, 55 (1), pp.015001. 10.1088/1361-6455/ac3f98 . hal-03851315

HAL Id: hal-03851315

<https://hal.science/hal-03851315v1>

Submitted on 21 Nov 2022

HAL is a multi-disciplinary open access archive for the deposit and dissemination of scientific research documents, whether they are published or not. The documents may come from teaching and research institutions in France or abroad, or from public or private research centers.

L'archive ouverte pluridisciplinaire **HAL**, est destinée au dépôt et à la diffusion de documents scientifiques de niveau recherche, publiés ou non, émanant des établissements d'enseignement et de recherche français ou étrangers, des laboratoires publics ou privés.



Distributed under a Creative Commons Attribution - NonCommercial - NoDerivatives 4.0
International License

The angular pattern in the hyperfine structure of Xe I and Kr I atoms

C Blondel and C Drag

Laboratoire de Physique des plasmas, Centre national de la recherche scientifique, Observatoire de Paris, Sorbonne Université, Université Paris-Saclay, École polytechnique, Institut polytechnique de Paris, route de Saclay, F-91120 Palaiseau, France

E-mail: christophe.blondel@lpp.polytechnique.fr

Abstract.

Recent reviews of the hyperfine structure of xenon and krypton have highlighted the variety of the values taken by the hyperfine coefficients A and B of these atoms. These variations, as functions of the atomic angular momenta, were however not explained quantitatively. This article shows the simple picture and angular momentum algebra that make it possible to account for the observed trend. The only necessary approximations are to consider the interaction of the outer electron negligible with respect to the coupling of the p^5 core with the nucleus, and to assume that the Racah $|(p^5)_j \ell[K]_J F\rangle$ basis, conventionally used for the atomic states of noble gases, makes a fitting description of the hierarchy of their angular momentum couplings. The way the calculation corroborates the apparently erratic values of hyperfine coefficients A and B in Xe I and Kr I shows up as a confirmation of the validity of these approximations.

Submitted to: *J. Phys. B: At. Mol. Phys.*

1. Introduction

^{129}Xe and ^{131}Xe , with abundances of 26% and 21%, are the only naturally occurring odd isotopes of Xe, and the only ones with a non-zero nuclear spin, $I = 1/2$ and $3/2$, respectively. Their hyperfine structure, which makes each of their fine-structure levels typically a doublet or a quartet, respectively, (except for those levels with a low J -value that restricts the set of allowed F values), has been the subject of many investigations. The corresponding results have been conveniently listed by Kono et al. (2013) and Kono et al. (2016), after extended investigations of the hyperfine structure of an unprecedentedly large number of excited levels of Xe. In their conclusions, however, these authors comment that “... the various smaller negative and positive values of A^{129} found in some Rydberg levels of neutral Xe may be envisaged simplistically as arising from angular-momentum dependent interactions between the Xe^+ ionic core and the Rydberg electron” (Kono et al. 2013) and that “There does not appear to be any obvious pattern or trend in these values of A^{129} , A^{131} and B^{131} as a function of the angular momentum quantum numbers J , ℓ , and K ” (Kono et al. 2016).

The quantum numbers these authors refer to are the ones usually preferred for the description of one-electron excited levels of noble gases (Racah 1942), the complete set of which includes j for the angular momentum of the p^5 electronic core ($3/2$ or $1/2$ for ‘unprimed’ and ‘primed’ levels, respectively), ℓ for the orbital momentum of the optical electron, K for the sum of the former momenta, J for the total electron momentum including the outer electron spin, F for the global momentum including the nuclear spin and an α variable for the other necessary quantum numbers (including the principal quantum number n of the outer electron).

As a matter of fact, the main trend of the apparently patternless distribution of hyperfine parameters can be explained very simply, once one has realized that the main contribution to the hyperfine correction of excited energy levels comes from the coupling of the p^5 inner electron shell with the nuclear momentum, with a much smaller contribution of the outer electron (Lieberman 1969, Luc-Koenig 1972). Neglecting the latter and applying standard angular-momentum algebra, one can then demonstrate that a first-order estimate of the hyperfine parameters of all singly-excited levels can be deduced from a single pair of ionic-core hyperfine parameters, which determines the relative orders of magnitude of the hyperfine splittings by purely angular formulae. Our purpose is to recall the corresponding recipe, which was described half a century ago (Lieberman 1971*b*), and show how remarkably it still applies to an updated set of experimental data.

2. The hyperfine structure of noble gas atoms

2.1. Dipolar term

The main perturbation leading to hyperfine splitting of a supposedly isolated well-defined- J level is the interaction of the magnetic moment of the nucleus, itself

proportional to the nuclear spin \mathbf{I} , with the magnetic field produced both by the motion of the surrounding electrons and by their own magnetic moments. The interaction energy has the form of a $\mathbf{X} \cdot \mathbf{I}$ term, with \mathbf{X} a vector operator of the electronic subspace (Bauche-Arnoult & Bauche 1968, Childs 1974) and can be written:

$$\Delta W_D = \langle \alpha(j, \ell) K, J, F, M_F | \mathbf{X} \cdot \mathbf{I} | \alpha(j, \ell) K, J, F, M_F \rangle \quad (1)$$

The matrix element is of course M_F -independent. Following general properties of the products of tensor operators, it can be written as the product of two reduced matrix elements (Armstrong 1971a, Hecht 2000a):

$$\Delta W_D = (-1)^{(J+I+F)} \begin{Bmatrix} J & I & F \\ I & J & 1 \end{Bmatrix} \langle \alpha J || \mathbf{X} || \alpha J \rangle \langle I || \mathbf{I} || I \rangle \quad (2)$$

Expressing the 6- j coefficient and taking into account the fact that the second matrix element is the one of the nuclear moment itself, which is equal to $[I(I+1)(2I+1)]^{1/2}$ (Hecht 2000b), one can simplify the dipolar shift into

$$\Delta W_D = \frac{C}{2[J(J+1)(2J+1)]^{1/2}} \langle \alpha J || \mathbf{X} || \alpha J \rangle \quad (3)$$

with $C = F(F+1) - J(J+1) - I(I+1)$. This is the usual form $\Delta W_D = A(\alpha, J) \langle I \cdot J \rangle = A(\alpha, J) \frac{C}{2}$, with (Bauche-Arnoult & Bauche 1968)

$$A(\alpha, J) = \frac{\langle \alpha J || \mathbf{X} || \alpha J \rangle}{[J(J+1)(2J+1)]^{1/2}} \quad (4)$$

Here comes the assumption that the hyperfine coupling, in noble gas atoms, is mainly due to the coupling of the inner p^5 electron core with the nuclear spin, and that the outer electron only packs this hyperfine-coupled core in more global angular momentum states. In this model, the $\langle J || \mathbf{X} || J \rangle$ matrix element can be broken down (Judd 1998) as

$$\langle \alpha(j, \ell) K, J || \mathbf{X} || \alpha(j, \ell) K, J \rangle = (-1)^{(K+1/2+J+1)} (2J+1) \begin{Bmatrix} J & 1 & J \\ K & 1/2 & K \end{Bmatrix} \langle \alpha(j, \ell) K || \mathbf{X} || \alpha(j, \ell) K \rangle \quad (5)$$

and the latter reduced matrix element can itself be broken down as:

$$\langle \alpha(j, \ell) K || \mathbf{X} || \alpha(j, \ell) K \rangle = (-1)^{(j+\ell+K+1)} (2K+1) \begin{Bmatrix} K & 1 & K \\ j & \ell & j \end{Bmatrix} \langle \alpha(p^5)_j || \mathbf{X} || \alpha(p^5)_j \rangle \quad (6)$$

The product of equations (4), (5) and (6) already produces a proportionality rule between $A(\alpha, J)$ and $\langle \alpha(p^5)_j | \mathbf{X} | \alpha(p^5)_j \rangle$, which generalizes the last equation of Giacobino et al. (1977) (written for a d' state, i.e. with $j=1/2$ and $\ell=2$). According to the approximation made, the residual reduced matrix element $\langle \alpha(p^5)_j | \mathbf{X} | \alpha(p^5)_j \rangle$ does no longer involve anything else than the core states, which we shall signal by abbreviating it as $\langle (p^5)_j | \mathbf{X} | (p^5)_j \rangle$ (even though it still depends on the radial properties of the core electrons and not only their p character). Notably, the outer electron principal quantum number n has been eliminated, which establishes the n -independence of the hyperfine correction, in the proposed approximation.

Furthermore, the reduced matrix element $\langle (p^5)_j | \mathbf{X} | (p^5)_j \rangle$ of the dipole operator for a p vacancy with respect to a complete $(p^6)_0$ shell can be calculated as the one of a p electron (Hubbs et al. 1958) and related to a dipolar parameter A_j in the same way:

$$\langle (p^5)_j | \mathbf{X} | (p^5)_j \rangle = [j(j+1)(2j+1)]^{1/2} A_j \quad (7)$$

Finally, writing (Trees 1953)

$$A_j = \frac{\ell_c(\ell_c+1)}{j(j+1)} a_{\ell_c} \quad (8)$$

with ℓ_c the core electron orbital quantum number, one can relate all A coefficients to a single one-electron parameter a_{ℓ_c} . Taking into account the fact that $\ell_c=1$ directly for the sake of brevity, one can write the explicit dependence of A on the angular quantum numbers j , ℓ , K and J as

$$A [(p^5)_j \ell [K]_J] = \kappa(j, \ell, K, J) \times a_{\ell_c} \quad (9)$$

with

$$\kappa(j, \ell, K, J) = \frac{[4J(J+1) + 4K(K+1) - 3][K(K+1) + j(j+1) - \ell(\ell+1)]}{8J(J+1)K(K+1)j(j+1)} \quad (10)$$

A comparison of the obtained A parameters with the variations described by (10) will be the subject of section 3.

2.2. Electric quadrupole term

The second effect of the nuclear structure on atomic spectra originates in existence of a quadrupole moment of the nuclear charge distribution. In the same way as for the dipolar term with formula (2), the quadrupolar term of the hyperfine perturbation can be expressed as a product of reduced matrix elements, but with tensor operators of rank 2:

$$\Delta W_Q = (-1)^{(J+I+F)} \begin{Bmatrix} J & I & F \\ I & J & 2 \end{Bmatrix} \langle \alpha J | \mathbf{Y}^{(2)} | \alpha J \rangle \langle I | \mathbf{K}^{(2)} | I \rangle \quad (11)$$

where $\mathbf{K}^{(2)}$ is the rank 2 operator of the nuclear subspace that appears in the expression of the quadrupole moment of the nucleus (Armstrong 1971*b*), and $\mathbf{Y}^{(2)}$ is the corresponding rank 2 operator of the electronic subspace. The F -dependence can be put entirely in the same variable C as for the dipolar term, which makes it possible to write the quadrupolar term :

$$\Delta W_Q = B(\alpha, J) \frac{3C(C+1) - 4I(I+1)J(J+1)}{8I(2I-1)J(2J-1)} \quad (12)$$

with (Bauche-Arnoult & Bauche 1968)

$$B(\alpha, J) = 2I(2I-1) \left[\frac{J(2J-1)}{(J+1)(2J+1)(2J+3)} \right]^{1/2} \langle \alpha J || \mathbf{Y}^{(2)} || \alpha J \rangle \quad (13)$$

Again relying on the hypothesis that the hyperfine energy essentially comes from the coupling of the nucleus with the p^5 electron core, one can unpack the quadrupolar matrix element $\langle \alpha J || \mathbf{Y}^{(2)} || \alpha J \rangle$ in the same way as the dipolar one, except for the replacement of the explicit rank 1 by a 2:

$$\begin{aligned} \langle \alpha(j, \ell) K, J || \mathbf{Y}^{(2)} || \alpha(j, \ell) K, J \rangle = \\ (-1)^{(K+1/2+J+2)} (2J+1) \begin{Bmatrix} J & 2 & J \\ K & 1/2 & K \end{Bmatrix} \langle \alpha(j, \ell) K || \mathbf{Y}^{(2)} || \alpha(j, \ell) K \rangle \end{aligned} \quad (14)$$

then

$$\begin{aligned} \langle \alpha(j, \ell) K || \mathbf{Y}^{(2)} || \alpha(j, \ell) K \rangle = \\ (-1)^{(j+\ell+K+2)} (2K+1) \begin{Bmatrix} K & 2 & K \\ j & \ell & j \end{Bmatrix} \langle (p^5)_j || \mathbf{Y}^{(2)} || (p^5)_j \rangle \end{aligned} \quad (15)$$

As for the dipolar coefficient, one could go one step further and take advantage of the fact that the quadrupolar term is a purely orbital one (entirely due to the coupling of the nuclear quadrupole with the quadrupolar term of the electron charge distribution) to write the last reduced matrix element as a purely orbital function. Of the two possible j values of the ionic core, however, only the higher $j = 3/2$ one can accommodate a non-zero quadrupole. In the proposed approximation, all ‘‘primed’’ levels shall thus have a zero quadrupolar term, so the question of having a formula for B applies only for one j value, which makes further decoupling unnecessary. For the corresponding ‘‘unprimed’’ states, $B(\alpha, j, \ell, K, J)$ thus appears proportional to the $\langle (p^5)_j || \mathbf{Y}^{(2)} || (p^5)_j \rangle$ reduced matrix element that would determine the quadrupole hyperfine coefficient B_j of the ground $j = 3/2$ state of $^{131}\text{Xe}^+$ in another application of formula (13):

$$B_j = 2I(2I-1) \left[\frac{j(2j-1)}{(j+1)(2j+1)(2j+3)} \right]^{1/2} \langle (p^5)_j || \mathbf{Y}^{(2)} || (p^5)_j \rangle \quad (16)$$

The ratio of formulae (13) and (16) gives a $\Lambda = B(\alpha, j, \ell, K, J)/B_j$ factor that describes all variations of the quadrupolar hyperfine coefficient $B(\alpha, j, \ell, K, J)$ for the singly excited states (for which j remains equal to $3/2$), with no dependence on the nuclear spin I left, as for the κ coefficient given by (10):

$$\begin{aligned} \Lambda(j, \ell, K, J) = & \left(j(j+1) [3(j^2 + j - 1) - 6\ell(\ell + 1) + 2K(K + 1)] \right. \\ & \left. + 3\ell(\ell + 1) [\ell^2 + \ell + 1 - 2K(K + 1)] + 3K(K + 1)(K^2 + K - 1) \right) \\ \times & \frac{24 [K(K + 1)(2K^2 + 2K - 5) + J(J + 1)(2J^2 + 2J - 5)] + 32J(J + 1)K(K + 1) + 63}{64 j(2j - 1)K(K + 1)(2K + 3)(2K - 1)(J + 1)(2J + 3)} \end{aligned} \quad (17)$$

The $\Lambda(j, \ell, K, J)$ ratio so obtained takes values in the interval $[-1, +1]$, the larger the orbital angular momentum ℓ the closer to the one or the other extreme. Remarkably enough, when all internal momenta align to produce a maximum value of J (i.e. when $J = \ell + 2$) Λ is always equal to 1, which makes the B parameter exactly equal to the one of the ion, in the model where all of the hyperfine coupling is due to the ionic core.

3. Comparison with calculated and experimental data

3.1. General comparison for xenon

3.1.1. Dipolar parameter Figure 1 shows how the $A [(5p^5)_j \ell [K]_J]$ parameter tabulated by Kono et al. (2016) compares to the theoretical κ coefficient given by formula (10). When nearly identical measurements have been made for the same A parameter, the plot is made for a single average value. The set has been complemented with the $^{129}\text{A} [5d[5/2]_2]$ coefficient measured by Cahuzac & Vetter (1975), the A values measured by Liberman (1969) and Liberman (1971a) for the $5d[1/2]$ and $5d[7/2]$ levels, the $^{131}\text{A} [7p[5/2]_2]$ value of Binet et al. (1983) and data from Liberman (1969), Jackson & Coulombe (1973), D’Amico et al. (2000), Brandi et al. (2001) and Suzuki et al. (2002) for $j = 1/2$ “primed” levels. As a general trend, the hyperfine parameter $A [(p^5)_j \ell [K]_J]$ appears to follow a clear proportionality rule with respect to κ , in quite a convenient first-order approximation.

An exception can be expected for levels with an outer s electron, which can come close to the nucleus and get coupled with the nuclear spin in a way quantitatively comparable to the core-hfs coupling. Significant deviation from the general trend actually appears for both $6s[3/2]_J$ levels. Parametric studies have demonstrated, however, that the $6s'[1/2]_1$ level owes much of its peculiarity to a strong mixing with the $5d[1/2]_1$ one (Coulombe & Sinzelle 1975). Conversely, the $nd[1/2]_1$ series has been analysed as an “extremely perturbed” one, the very diverse A values of which have been attributed to strong variations in the actual angular momentum coupling scheme and to configuration mixing (Coulombe 1975). These perturbations of the $nd[1/2]_1$ and

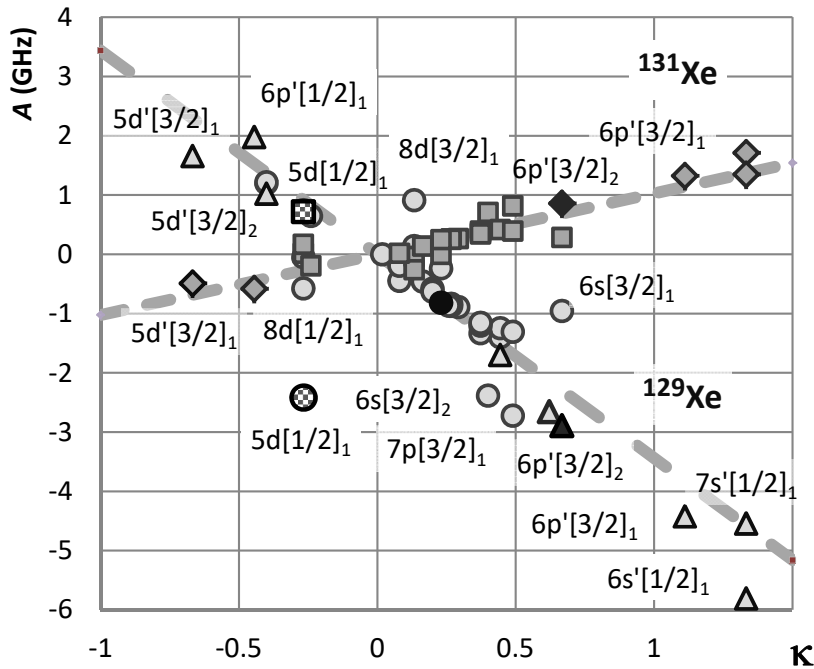


Figure 1. Dipolar hyperfine coefficients $A [(5p^5)_j \ell [K]_J]$ of ^{129}Xe (circles and triangles) and ^{131}Xe (squares and diamonds) shown vs. their expected κ ratio to the mono-electronic a_{l_c} parameter. Circles and squares (resp. triangles and diamonds) stand for the $j=3/2$ “unprimed” (resp. $j=1/2$ “primed”) levels. Most data are taken from table 2 of Kono et al. (2016), with complements from a few other references, including the $^{129}\text{A} [5d[5/2]_2]$ value measured by Cahuzac & Vetter (1975) (represented with the black disk) and the $A [5d[1/2]_1]$ values of Liberman (1969) and Liberman (1971a) (the markers of which are singled out by chequered filling). The black triangle and diamond show the positions of the $A [6p'[3/2]_2]$ coefficients of ^{129}Xe and ^{131}Xe , respectively, which were measured (one more time) during our recent investigation of the two-photon excitation cross-section of Xe. The dashed and short-dashed lines show the general trend of the ^{129}A and ^{131}A coefficients to follow a linear dependence with respect to the angular κ factor deduced from the hypothesis of a pure core-hfs effect.

$nd[3/2]_1$ series are made conspicuous by the Lu-Fano plot of the odd $J=1$ states of Xe I (Geiger 1977), where both the $8d[1/2]_1$ and $8d[3/2]_1$ appear strongly perturbed by the vicinity of the $5d'[3/2]_1$ level. Numerically, the most perturbed $5d[1/2]_1$ level was found to be only in a proportion smaller than 53% what the Racah notation supposes and to contain as much as 28% of a $j=1/2$ “primed” component (Liberman 1971b).

The apparent zero value of $A [(5p^5)_{3/2} f[5/2]_2]$ (this is, in figure 1, the point closest to the origin) led Kono et al. (2016) to wonder “how unusual” it could be to have an A parameter “accidentally indistinguishable from zero”. The explanation stems directly from the very low value of $\kappa (f[5/2]_2) = 4/225$, which is apparently to be passed, for reasonably small values of ℓ (all limits of κ , whatever the accompanying values of K and J , are zero when ℓ tends to infinity), only by $\kappa (f[5/2]_3) = 4/315$. As far as we know, no experiment ever investigated the hyperfine structure of the latter nf series, but

multiconfiguration Dirac-Hartree-Fock (MCDHF) calculations actually confirmed that all six $4f[5/2]_J$, $5f[5/2]_J$ and $6f[5/2]_J$ levels should have especially small A dipolar coefficients (Salah & Hassouneh 2019, Hassouneh & Salah 2020). As functions of the ℓ variable, the twin series $\kappa(\ell[K=\ell-1/2]_J)$ appear to be the only ones that have κ virtually cross the $\kappa=0$ axis and change its sign, and that occurs between values 3 and 4 of the ℓ variable, hence making the $\kappa(f[5/2]_J)$ and $\kappa(g[7/2]_J)$ terms particularly small ones. As concerns the latter, this has been confirmed by the A values found numerically for both $^{129}\text{A}[5g[7/2]_J]$ coefficients (Hassouneh et al. 2020). And that also explains the weakness of $A[6d[3/2]_2]$, which corresponds to the very preceding term in one of the $\kappa(\ell[K=\ell-1/2]_J)$ series just considered, with a κ value of $2/25$.

To answer the question completely, examination of equation (10) shows that there are no finite values of the angular momenta that make κ strictly equal to zero.

A more quantitative analysis lies beyond the scope of the present work, the aim of which is just to show that a first-order of magnitude of the hyperfine structure can be given by a very simple non-relativistic treatment. Parametric analyses have emphasized that a complete understanding of the hyperfine structure of xenon cannot be achieved without taking into account numerically configuration interactions and relativistic effects (Liberian 1969, Luc-Koenig 1972, Coulombe & Sinzelle 1975).

3.1.2. Quadrupolar parameter Quadrupolar parameters read from table 2 of Kono et al. (2016) and complemented by the experimental data of Liberman (1971a) for the $5d[1/2]_1$ and $5d[3/2]_2$ levels are plotted in a similar way in figure 2. Again due to strong mixing with other series, the effect of which has already been described on the dipolar coefficient, the $nd[1/2]_1$ series significantly departs from the zero quadrupolar moment it would have if all of its levels were actually pure $K=1/2$ ones. As already observed with the dipolar coefficient too, the $8d[3/2]_1$ level appears substantially perturbed by the vicinity of the $5d'[3/2]_1$ level, the ^{131}B coefficient of which has been found significantly different from zero (Brandi et al. 2001), due to its own mixing with $j=3/2$ states.

Apart from these particular cases, the quadrupolar coefficient ^{131}B appears essentially proportional to the angular parameter Λ that relates the total angular momentum to the angular momentum of the $(5p^5)_{3/2}$ core, in Racah's coupling scheme, as concerns quadrupole coupling to the nuclear charge distribution. The "pattern" of large, small, positive or negative hyperfine B parameters appears thus definitely determined by formula (17) and, contrary to the dipolar coefficient, this is true even for s states, for an s state cannot have but a zero quadrupolar moment (hence leaving the whole quadrupolar coupling to the p^5 core). Remarkably enough, the maximum value of coefficient Λ is reached by all states that correspond to a maximum of the total angular momentum, for a given ℓ value. These states, such that $J=K+1/2=\ell+2$, all have the same $\Lambda=1$. This is the reason why the $6s[3/2]_2$ and $6p[5/2]_3$ levels have nearly identical B parameters, which are also the largest ones.

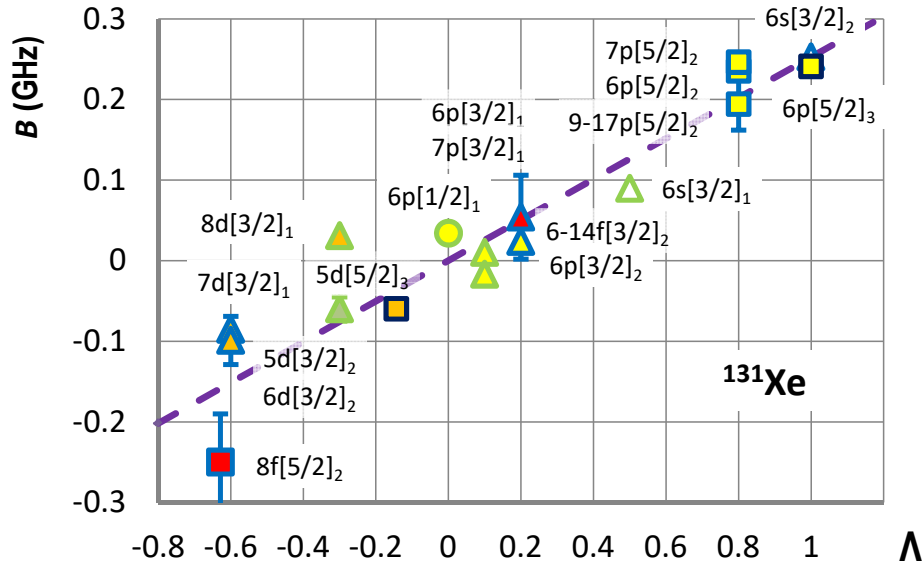


Figure 2. Quadrupolar parameters $^{131}B[(5p^5)_j\ell[K]_J]$ of ^{131}Xe , shown vs. their expected Λ ratio to the quadrupolar parameter $^{131}B_{3/2}$ of the ionic $(5p^5)_{3/2}$ core. The inner colour (online) of the markers is white, yellow, orange or red for s , p , d and f levels respectively, the outer colour is green, blue or dark blue for $J = 1, 2$ and 3 levels respectively, the markers themselves are circles, triangles or squares for $K = 1/2, 3/2$ and $5/2$ levels, respectively. The dashed line shows the trend of the ^{131}B coefficient to follow a linear dependence with respect to the angular Λ factor established on the hypothesis of a pure core-hfs effect. The observed slope of 253 MHz corresponds to the known value of the quadrupolar parameter B of $^{131}\text{Xe}^+$.

3.1.3. Accuracy of the hyperfine parameters - the example of the $6p'[3/2]_2$ level In addition to the particularities just noted, one should emphasize that the larger or smaller deviations of A and B parameters from the average behaviour made conspicuous on figures 1 and 2 are not noise, or the result of large uncertainties on the measured hyperfine parameters. Those parameters have actually been measured with such precisions that, in most cases, uncertainty bars are too small to be represented on the figures.

An example of the achieved precision can be given with the hyperfine structure of the $6p'[3/2]_2$ level, which appears in a two-photon absorption laser induced fluorescence (TALIF) spectrum (figure 3) that we recorded recently as a sideline, while measuring the two-photon excitation cross-sections of the $6p'[3/2]_2$ and $6p'[1/2]_0$ levels of xenon (Drag et al. 2021).

The hyperfine parameters of the $6p'[3/2]_2$ level (the $6p'[1/2]_0$ of course has no hyperfine structure) had already been measured many times, leading to a series of experimental values shown in table 1. We have obtained $^{129}A = -2880(15)$ MHz, which appears compatible with all previous measurements. Even in a Doppler-free configuration, however, two-photon absorption spectroscopy cannot be as precise as the

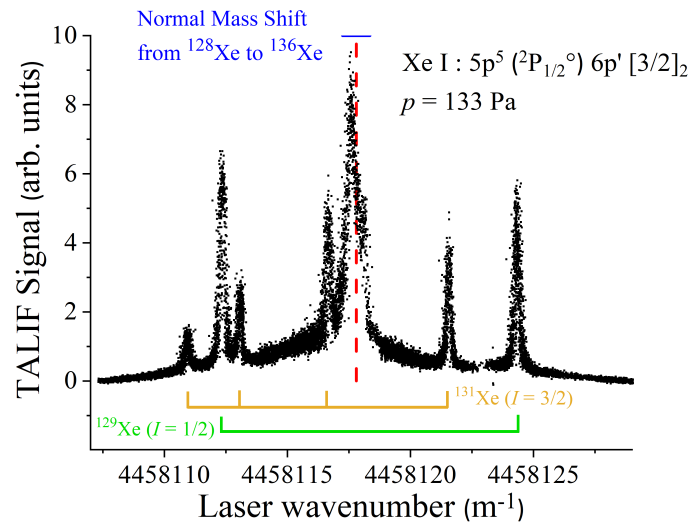


Figure 3. Example of a hyperfine multiplet, recorded as a fluorescence spectrum following two-photon excitation, in a Doppler-free configuration, of the $6p'[3/2]_2$ level of xenon. The grouped single lines of the even isotopes are found around the expected laser wavenumber 4458117.8 m^{-1} , the position of which is indicated by a dashed vertical line. The horizontal line, above the group, shows the interval spanned by the normal mass shift. The hyperfine doublet and quadruplet structures of ^{129}Xe and ^{131}Xe , respectively, are designated by the vertical lines below.

Table 1. Hyperfine dipole parameter of the $6p'[3/2]_2$ level of ^{129}Xe I (MHz).

| ^{129}A | Reference |
|--------------|--|
| -3000(100) | Jones (1934), Kopfermann & Rindal (1934) |
| -2897(13) | Bohr et al. (1952) |
| -2892.7(3.0) | Jackson & Coulombe (1972) |
| -2891.5(6.0) | Jackson & Coulombe (1973) |
| -2894.6(4.7) | Suzuki et al. (2002) |
| -2889(4) | Pawelec et al. (2011) |
| -2875 | Parametric study by Liberman (1969) |
| -2865.9478 | MCDHF by Salah & Hassouneh (2019) |
| -2880(15) | Present work |

most recent investigations of the hyperfine structure *per se*, which relied on one-photon saturated absorption (Suzuki et al. 2002, Pawelec et al. 2011).

Under the assumption of pointlike nuclei, the dipolar coefficient ^{131}A of isotope 131 can be directly deduced from the one of the lighter isotope, for $I \times A$ then just varies in proportion of the nuclear magnetic moment, which entails $^{129}A/^{131}A \simeq -3.3734$ (Kono et al. 2013). Relying on the known value of ^{129}A , one thus expects $^{131}A [6p'[3/2]_2] \simeq 857\text{ MHz}$. The results of successive measurements, together with the experimental value of the quadrupolar parameter, are shown in table 2.

Table 2. Hyperfine parameters of the $6p'[3/2]_2$ level of ^{131}Xe I (MHz).

| ^{131}A | ^{131}B | Reference |
|------------|-----------|--|
| 857(2) | | Expected from the mean value of ^{129}A |
| 835(13) | -45(30) | Bohr et al. (1952) |
| 858.9(3.1) | -14(17) | Suzuki et al. (2002) |
| 829(4) | 72(17) | Pawelec et al. (2011) |
| | -12(18) | Parametric calculation by Liberman (1971a) |
| 858.37 | -17.96 | MCDHF by Hassouneh & Salah (2020) |
| 853(17) | -31(85) | Present work |

If level $6p'[3/2]_2$ was actually a pure ‘prime’, i.e. a level for which the $5p^5$ core can be characterized by a $j = 1/2$ angular momentum, in the proposed approximation where the hyperfine structure is supposed to stem essentially from the hyperfine structure of the core, the quadrupolar term would be zero. Relativistic effects, however, make the picture less simple and parametric calculations have shown the core of $6p'[3/2]_2$ states to be made only by 90% of real ‘prime’ states, i.e. with a $j = 1/2$ core (Liberman 1969), the remaining part consisting of a nearly 10% admixture of $(5p^5)_{j=3/2}[3/2]_2$ states (Liberman 1971b). Experimentally, we have obtained $^{131}A = 853(17)$ and $^{131}B = -31(85)$ MHz, with a +0.37 correlation coefficient between the associated uncertainties. Our ^{131}A value thus appears very close to the weighted average of former measurements 847(3) MHz, but its rather large uncertainty prevents it from being really informative. Nevertheless, our measured value for $^{131}B[6p'[3/2]_2]$, together with the more recent calculation (Hassouneh & Salah 2020), tends to confirm that obtaining a positive B -value for that level (Pawelec et al. 2011) probably resulted from some misinterpretation.

3.2. A comparison for krypton

3.2.1. Dipolar parameter The comment that some “trends in A and B values for ^{83}Kr (...) differ markedly from their counterparts for ^{129}Xe and ^{131}Xe ” (Kono et al. 2016) makes it worth carrying out a similar analysis for ^{83}Kr . Figure 4 shows how faithfully the dipolar parameter of ^{83}Kr I also follows the general trend indicated by formula (10). Strikingly enough, the few levels that deviate substantially from the linear trend appear to belong to the same series as in Xe I, namely the $d[1/2]_1$, $s[3/2]$ and $s'[1/2]_1$ ones. Despite the fact the hyperfine perturbation is one order of magnitude smaller than in Xe, most relative deviations appear to be of the same sign and order of magnitude in the one and the other atom, which invalidates the negative statement just quoted. On the contrary, all observed trends appear very similar.

3.2.2. Quadrupolar parameter Figure 5 shows how the B parameter of ^{83}Kr follows the trend set by the Λ coefficient of formula (17). In the same way as for ^{131}Xe , all levels with a maximum angular momentum $J = K + 1/2 = \ell + 2$ are predicted to have

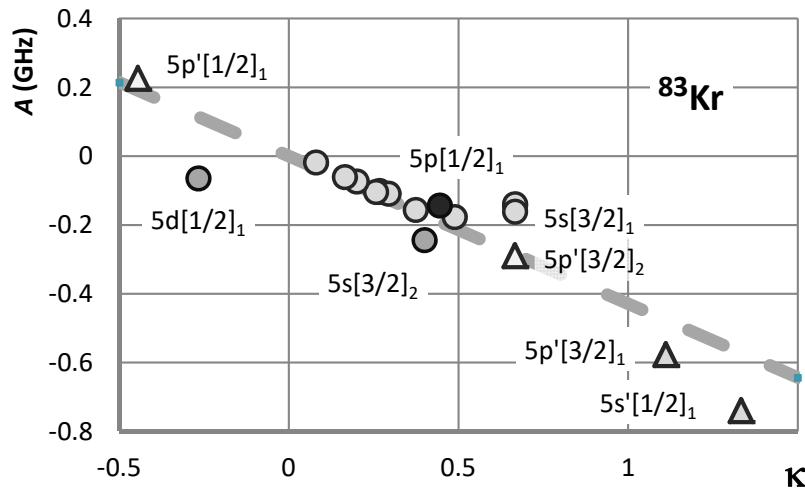


Figure 4. Dipolar hyperfine coefficients ${}^{83}A [(4p^5)_j \ell [K]_J]$ of ${}^{83}\text{Kr}$ shown vs. their expected κ ratio to the mono-electronic $a_{\ell c}$ parameter. Circles (resp. triangles) stand for the $j = 3/2$ “unprimed” (resp. $j = 1/2$ “primed”) levels. ${}^{83}A$ parameters for states with a $j = 3/2$ core taken from Kono et al. (2016) are complemented with the ${}^{83}A [5p[1/2]_1]$ value (represented by the black disk) measured by Safia & Husson (1984). The data for the core-excited $j = 1/2$ “primed” levels are taken from Jackson (1977), Husson et al. (1979), Cannon (1993) and Silwal & Brandenberger (2006). The dashed line shows the general trend of ${}^{83}A$ to follow a linear dependence with respect to the κ factor deduced from the hypothesis of a pure core-hfs effect.

a maximum B value, which actually leads to an accumulation of data points at the abscissa $\Lambda = 1$. One of the largest deviations from the pure core-hfs model logically occurs for an s -level, namely $5s[3/2]_1$, with a relative reduction with respect to the expected value quite similar to the one observed with the $6s[3/2]_1$ of Xe I. Levels with larger principal quantum numbers, in the same series, appear to be much closer to the model. The surprise comes from the $5d[3/2]_2$ level, the B parameter of which appears completely inverted with respect to the prediction of the pure core-hfs model. As a matter of fact, multichannel quantum-defect (MQDT) analysis of the odd-parity $J = 2$ spectrum of neutral krypton has shown that both adjacent $5d[3/2]_2$ and $5d[5/2]_2$ undergo a large perturbation due to the vicinity of the core-excited $4d'[3/2]_2$ and $4d'[5/2]_2$ levels (Aymar et al. 1981). An even larger perturbation of the energy levels occurs with the $8d[3/2]_2$, which is repelled above the $8d[5/2]_2$ by the $5d'[3/2]_2$ and $5d'[5/2]_2$ ones (Aymar et al. 1981). Unfortunately we have no hyperfine measurement for the $8d[3/2]_2$ level.

The complexity of the resulting four-series mixing explains that, in such a situation, no hyperfine coefficient can be predicted in a simple way ; Λ takes a negative value for the $d[5/2]_2$ coupling as for the $d[3/2]_2$ one (and a zero value for all $j = 1/2$ core-excited states), which does not make the change of sign observed in ${}^{83}B [5d[3/2]_2]$ intuitive. The reasons why no anomaly has appeared on the dipolar coefficient ${}^{83}A [5d[3/2]_2]$ may be that i) $\kappa(d[3/2]_2)$ has a particularly small value and that ii) the potentially

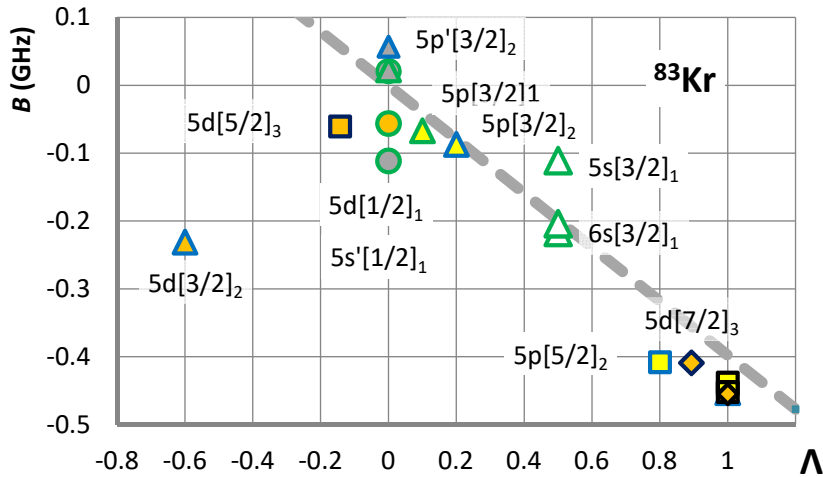


Figure 5. Quadrupolar parameters ${}^{83}B[(4p^5)_j\ell[K]_J]$ of ${}^{83}\text{Kr}$, shown vs. their expected Λ ratio to the quadrupolar parameter ${}^{83}B_{3/2}$ of the ionic $(4p^5)_{3/2}$ core. The inner colour (online) of the markers is white, yellow, or orange for s , p and d levels respectively, except for the core-excited “primed” levels, the $j = 1/2$ core momentum of which makes $\Lambda = 0$, which have been uniformly filled in grey. The outer colour is green, blue, dark blue or black for $J = 1, 2, 3$ and 4 levels respectively, the markers themselves are circles, triangles, squares or diamonds for $K = 1/2, 3/2, 5/2$ and $7/2$ levels, respectively. The dashed line shows the trend of ${}^{83}B$ to follow a linear dependence with respect to the angular Λ factor established on the hypothesis of a pure core-hfs effect. The observed slope of -398 MHz roughly corresponds to the known value of the quadrupolar parameter B of ${}^{83}\text{Kr}^+$.

contaminating $\kappa(d'[3/2]_2)$ and $\kappa(d'[5/2]_2)$ coefficients have strong values, $-2/5$ and $+28/45$ respectively, but with opposite signs. The experimentally negative value of -231 MHz found for ${}^{83}B[5d[3/2]_2]$ (Silwal & Brandenberger 2006) has been confirmed, anyway, by MCDHF calculations, which found -229 MHz (Salah & Hassouneh 2018). These calculations also confirmed the localised character of the anomaly, since they found the $6d[3/2]_2$ and $7d[3/2]_2$ terms of the series to have perfectly normal $\Lambda(\frac{3}{2}, 2, \frac{3}{2}, 2)$ -proportional B coefficients, with values of 243 and 249 MHz, respectively.

The deviation from the general trend observed with the $5d[5/2]_3$ and, to a lesser extent, with the $5d[7/2]_3$ level may be linked to the observation that the $J = 3$ series are, on average, made of less purely $|j\ell[K]_J\rangle$ states than the ones with a total angular momentum $J = 1$ or $J = 2$. The special behaviour of the $5d[5/2]_3$ may also owe something to its proximity with the $5d[7/2]_3$ and $4d'[5/2]_3$ levels, the perturbing effect of which also clearly appears on the Lu-Fano plot (Aymar et al. 1981).

4. Directions for a thorough analysis of the hyperfine structure

As emphasized in section 3.1.1, a really quantitative analysis of the hyperfine structure of the heavier noble gases must resort to a relativistic description and take configuration

interactions into account. Even though plotting the hyperfine A and B coefficients as functions of the angular coupling coefficients κ and Λ makes it conspicuous that most of the observed hyperfine structure stems from the coupling of the ionic core with the nucleus, relying on the average values of the A/κ or B/Λ ratios to determine the hyperfine coefficient of the ion can only be a crude method.

For instance, using formula (8), one can translate the $^{129}a_{\ell_c} \simeq -3439$ MHz value given by the linear regression represented on figure 1 into values of the dipolar coefficient for one and the other fine-structure level of the $^{129}\text{Xe}^+$ ionic core, numerically $^{129}A_{3/2} \simeq -1834$ MHz and $^{129}A_{1/2} \simeq -9171$ MHz, with, automatically, a 1:5 ratio (Bauche-Arnoult & Bauche 1968). On the other hand, separate linear regressions for the one and the other j values yield $^{129}A_{3/2} \simeq -1375$ MHz and $^{129}A_{1/2} \simeq -10253$ MHz, i.e. a 1:7.5 ratio. Since they do not make use of the approximation formula (8) is based on, the latter results may be considered more realistic. This seems confirmed, at least for the $A_{3/2}/A_{1/2}$ ratio, when configuration interactions are taken into account in a relativistic description (Coulombe & Sinzelle 1975) and by the MQDT analysis of the evolution of the hyperfine structure along the Rydberg series (Schäfer et al. 2010). The produced values of $^{129}A_{3/2} \simeq -1.65$ GHz and $^{129}A_{1/2} \simeq -12.1$ GHz are actually in a 1:7.4 ratio.

The fact that the absolute values of A found by the more accurate methods are significantly larger, and the example of krypton show, however, that this quantitative agreement may have been obtained only by chance. The one-parameter analysis materialized by the dashed line of figure 4 yields -229 and -1144 MHz, for the $^{83}A_{3/2}$ and $^{83}A_{1/2}$ dipolar coefficients of $^{83}\text{Kr}^+$, respectively. These are not too far from the more exact, although more contrasted values of -198 and -1199 MHz produced by the MQDT analysis (Schäfer & Merkt 2006). Separate linear regressions on the $j=3/2$ and $j=1/2$ data of figure 4, however, yield consistent values only when the perturbed $s[3/2]_1$ and $d[1/2]_1$ levels are removed from the sample. With this somewhat arbitrary clean-up, the obtained $^{83}A_{3/2}$ and $^{83}A_{1/2}$ coefficients, -215 and -1401 MHz, respectively, do not appear much more accurate than the ones produced by the one-dimensional model. Correct orders of magnitude are nevertheless produced, for both atoms, by the simplest model.

Ionic quadrupolar coefficients obtained by linear regression of data such as the ones of figures 2 and 5 may also be interesting. Remarkably, the $^{131}B_{3/2} = 252.51(2)$ MHz obtained from figure 2 for the $^{131}\text{Xe}^+$ ion agrees nearly perfectly with the 252.52(1) MHz once measured on the $6s[3/2]_2$ level of Xe I (Faust & McDermott 1961). Meanwhile, a subsequent parametric analysis has produced two slightly different values of $^{131}B_{3/2}$, 280 or 245 MHz, depending on whether it was based on the spectroscopy of even or odd levels, respectively, which was interpreted as a consequence of the imperfections of far configuration interaction modelling (Lieberman 1971*a*). The MQDT analysis gave 260.48(25) MHz (Schäfer et al. 2010). This, again, illustrates the limitations of a first-order model and the need for more elaborate descriptions.

A similar comparison can be made, for the case of ^{83}Kr , between the $^{83}B_{3/2} \simeq -398$ MHz slope of figure 5 and the $^{83}B_{3/2} = -381(13)$ MHz ionic parameter produced by an MQDT analysis (Wörner et al. 2003). Our first-order approximation thus appears

quite correct, as far as the order of magnitude of B is concerned, but again, cannot substitute for more elaborate analyses, the implementation of which is beyond the scope of the present work. As an illustration of the intricacies of the problem, millimetre-wave spectroscopy together with multichannel quantum-defect-theory later revised the latter figure substantially, to ${}^{83}B_{3/2} = -462(22)$ MHz (Schäfer & Merkt 2006).

5. Conclusion

The variations of dipolar and quadrupolar hyperfine parameters of Xe and Kr have been shown to obey, at first order, simple angular formulae based on the assumption that most of the hyperfine coupling is due to the interaction of the $(p^5)_j$ core with the nucleus. The situation appears thus indeed opposite to the one of alkali atoms, the $j=0$ core of which can of course not undergo any hyperfine coupling, thus making the outer electron the only source of hyperfine structure. In noble gas atoms, in contradistinction, the hyperfine coupling of the outer electron with the nucleus appears a lot weaker than the core-nucleus coupling. With this physical image of a pure core-hfs coupling in mind, it is thus no wonder that the hyperfine coefficients of Xe and Kr exhibit nearly no dependence on the principal quantum number n of the outer electron, except for the members of the Rydberg series located in the vicinity of a core-excited perturber. Those exceptions are illustrated by the extraordinary ${}^A A$ values of the $5d[1/2]_1$ level of Xe I and ${}^{83}B$ value of the $5d[3/2]_2$ level of Kr I, which have been explained by both a significant deviation from the Racah coupling scheme and configuration mixing. Apart from these exceptions, all relative variations of the hyperfine coefficients of singly excited states of Kr I and Xe I, which seemed so patternless to Kono et al. (2016), can be explained or predicted by simple angular-momentum algebra. Plotting the experimental hyperfine parameters as functions of the angular coefficient calculated in this way provides sensible estimates of the hyperfine coefficients of the ionic core. Accurate measurements of the latter can only be obtained, however, by more elaborate models.

Acknowledgments

This article is dedicated to the memory of René-Jean Champeau, who passed away July 19, 2021. Professor Champeau's own contributions to hyperfine spectroscopy (Champeau & Gerstenkorn 1960, Champeau 1964, Champeau et al. 1973, Champeau et al. 1974) made him an expert, whose kind support was of great value when preparing this article. We here express our deep appreciation for the sound advice he generously gave us for decades, not only on atomic spectroscopy, but more generally on physics and the way to teach and understand it.

References

- Armstrong L 1971*a* *Theory of the hyperfine structure of free atoms* Wiley. Formula II-24.
 Armstrong L 1971*b* *Theory of the hyperfine structure of free atoms* Wiley. Chapter IV.

- Aymar M, Robaux O & Thomas C 1981 *J. Phys. B: At. Mol. Phys.* **14**, 4255.
- Bauche-Arnoult C & Bauche J 1968 *Ann. Phys.-Paris* **14**, 341.
- Binet G, Husson X & Grandin J P 1983 *J. Phys. Lett. (Paris)* **44**, 151.
- Bohr A, Koch J & Rasmussen E 1952 *Ark. Fys.* **4**(29), 455.
- Brandi F, Velchev I, Hogervorst W & Ubachs W 2001 *Phys. Rev. A* **64**, 032505.
- Cahuzac P & Vetter R 1975 *Phys. Rev. Lett.* **34**, 1070.
- Cannon B D 1993 *Phys. Rev. A* **47**, 1148.
- Champeau R J 1964 *J. Phys. (Paris)* **25**, 825.
- Champeau R J & Gerstenkorn S 1960 *C. R. Hebd. Acad. Sci.* **251**, 352.
- Champeau R J, Handrich E & Walther H 1973 *Z. Phys.* **260**, 361.
- Champeau R J, Keller J C, Robaux O & Vergès J 1974 *J. Phys. B: At. Mol. Phys.* **7**, L163.
- Childs W J 1974 in 'Case studies in atomic physics' Vol. 3 Elsevier p. 215.
- Coulombe M 1975 'Contribution à l'étude du déplacement isotopique et de la structure hyperfine dans le spectre d'arc du xénon' thèse de doctorat d'État ès sciences physiques. Faculté des sciences d'Orsay.
- Coulombe M C & Sinzelle J 1975 *J. Phys. (Paris)* **36**, 773.
- D'Amico G, Pesce G & Sasso A 2000 *Hyperfine Interact.* **127**, 121.
- Drag C, Marmuse F & Blondel C 2021 *Plasma Sources Sci. Technol.* **30**, 075026.
- Faust W L & McDermott M N 1961 *Phys. Rev.* **123**, 198.
- Geiger J 1977 *Z. Phys. A* **282**, 129.
- Giacobino E, Biraben F, Grynberg G & Cagnac B 1977 *J. Phys. (Paris)* **38**, 623.
- Hassouneh O & Salah W 2020 *J. Quant. Spectrosc. Ra.* **255**, 107246.
- Hassouneh O, Salah W & Bathish S 2020 *Results Phys.* **16**, 102864.
- Hecht K T 2000a in 'Quantum Mechanics' Springer pp. 312–329. Chapter 34. Formula 28.
- Hecht K T 2000b in 'Quantum Mechanics' Springer pp. 299–302. Chapter 32. Formula 7.
- Hubbs J C, Marrus R, Nierenberg W A & Worcester J L 1958 *Phys. Rev.* **109**, 390.
- Husson X, Grandin J P & Kucal H 1979 *J. Phys. B: At. Mol. Phys.* **12**, 3883.
- Jackson D A 1977 *J. Opt. Soc. Am.* **67**, 1638.
- Jackson D A & Coulombe M C 1972 *P. Roy. Soc. Lon. A Mat.* **327**, 137.
- Jackson D A & Coulombe M C 1973 *P. Roy. Soc. Lon. A Mat.* **335**, 127.
- Jones E G 1934 *P. Roy. Soc. Lon. A-Conta.* **144**, 587.
- Judd B R 1998 *Operator techniques in atomic spectroscopy* Vol. 35 Princeton University Press. Formula 3.37.
- Kono M, He Y, Baldwin K G H & Orr B J 2013 *J. Phys. B: At. Mol. Opt. Phys.* **46**, 035401.
- Kono M, He Y, Baldwin K G H & Orr B J 2016 *J. Phys. B: At. Mol. Opt. Phys.* **49**, 065002.
- Kopfermann H & Rindal E 1934 *Z. Phys.* **87**, 460.
- Liberman S 1969 *J. Phys. (Paris)* **30**, 53.
- Liberman S 1971a *J. Phys. (Paris)* **32**, 867.
- Liberman S 1971b 'Études de structures hyperfines et d'effets isotopiques dans les raies laser infrarouges de gaz rares' thèse de doctorat d'État ès sciences physiques. Faculté des sciences d'Orsay.
- Luc-Koenig E 1972 *J. Phys. (Paris)* **33**, 847.
- Pawelec E, Mazouffre S & Sadeghi N 2011 *Spectrochim. Acta Part B* **66**, 470.
- Racah G 1942 *Phys. Rev.* **61**, 537.
- Safia H A & Husson X 1984 *J. Phys. (Paris)* **45**, 863.
- Salah W & Hassouneh O 2018 *J. Phys. Commun.* **2**, 035014.
- Salah W & Hassouneh O 2019 *Results Phys.* **12**, 153.
- Schäfer M & Merkt F 2006 *Phys. Rev. A* **74**, 062506.
- Schäfer M, Raunhardt M & Merkt F 2010 *Phys. Rev. A* **81**, 032514.
- Silwal R & Brandenberger J R 2006 *Phys. Rev. A* **73**, 032508.
- Suzuki M, Katoh K & Nishimiya N 2002 *Spectrochim. Acta Part A* **58**, 2519.
- Trees R E 1953 *Phys. Rev.* **92**, 308.

